Catalysis Science & Technology

Accepted Manuscript

Catalysis Science & Technology

ARTICLE TYPE

Cite this: DOI: 10.1039/c0xx00000x

www.rsc.org/xxxxxx

Silica coated magnetic Fe_3O_4 nanoparticles supported phosphotungstic acid: a novel environment-friendly catalyst for the synthesis of 5-ethoxymethylfurfural from 5-hydroxymethylfurfural and fructose

Shuguo Wang, Zehui Zhang*, Bing Liu and Jinlin Li

Received (in XXX, XXX) Xth XXXXXXXXX 20XX, Accepted Xth XXXXXXXXX 20XX
DOI: 10.1039/b000000x

In this study, a magnetically-recoverable catalyst (Fe_3O_4@SiO_2-HPW) was prepared by the application of phosphotungstic acid (HPW) supported on silica-coated Fe_3O_4 nanoparticles. The prepared samples were characterized by XRD, TEM, FT-IR, and N_2-adsorption-desorption isotherm. The content of W in Fe_3O_4@SiO_2-HPW was measured by inductively coupled plasma atomic emission spectroscopy (ICP-AES) and its surface acidity was determined by a potentiometric titration with *n*-butyl amine. Fe_3O_4@SiO_2-HPW showed an excellent catalytic activity for the synthesis of EMF from HMF and fructose. Under an optimal reaction conditions, EMF was obtained in a high yield of 83.6% by the etherification of 5-hydroxymethylfurfural. EMF could also be synthesized directly from fructose in a yield of 54.8% via a one-pot reaction strategy. After reaction, the catalyst Fe_3O_4@SiO_2-HPW could be easily separated from the reaction mixture with an external magnetic field, and it could be reused at least five times without any loss of its catalytic activity.

1. Introduction

With diminishing fossil fuel, much effort has been devoted to the production of fuels and chemicals from renewable sources.[1-3] Abundant, renewable biomass resource is a promising alternative to petroleum for production of chemicals and liquid fuels.[4-5] In recent years, various chemicals have been successfully synthesized from biomass. Among the many biomass-derived chemicals, 5-hydroxymethylfurfural (HMF) is considered an excellent platform molecule. HMF serves as a platform chemical for the production of a wide range of chemicals and biofuels, which can be converted to energy products (2,5-dimethylfuran),[6] monomers for high-value polymers (2,5-furandicarboxylic acid[7] and 2,5-hydroxymethylfuran[8]) and valuable intermediates for fine chemistry.[9] Therefore, extensive studies have been carried out for the transformation of carbohydrates and cellulosic biomass into HMF.[10-15]

5-Ethoxymethylfurfural (EMF), the etherification product of HMF, has been proposed as a potential liquid biofuel for the future.[16] EMF is presented in liquid with a high boiling point of 235 ^oC. It has a high energy density of 8.7 kWh/L, which is close to the standard gasoline (8.8 kWh/L).[17] EMF can be directly synthesized from HMF or 5-chloromethylfurfural (CMF) with high yields.[18-20] However, the large-scale synthesis of EMF from pure HMF or CMF is limited due to the high price of HMF and CMF. It is much more attractive to synthesize EMF from inexpensive and renewable fructose via a one-pot reaction strategy. As shown in scheme 1, the one-pot reaction integrates the dehydration of fructose into HMF and the followed etherification of HMF into EMF, which saves time and energy. In recent years, some methods were reported on the synthesis of EMF from fructose. Yang et al. reported that an EMF yield of 65% could be obtained from fructose in the presence of heteropolyacid $H_3PW_{12}O_{40}$ under microwave heating.[21] Kraus et al. reported that EMF could be achieved with an approximate yield of 55% from fructose catalyzed by acidic ionic liquids.[22] However, the procedures for the catalyst recycling of the above mentioned methods were complex, as $H_3PW_{12}O_{40}$ and acidic ionic liquids were dissolved in the solvents. Balakrishnan et al.

Dr. S.G. Wang, Dr. Z. H. Zhang, Dr. B. Liu, Prof. J. L. Li, Department of Chemistry, key Laboratory of Catalysis and Material Sciences of the State Ethnic Affairs Commission & Ministry of Education. South-Central University for Nationalities MinYuan Road 708, Wuhan, R.P. China Fax: (+)86-27-67842572 E-mail: zehuizh@mail.ustc.edu.cn

prepared a heterogeneous catalyst by the graft sulfuric acid on the surface of silica, and it showed high catalytic activity on the synthesis of EMF from fructose with a yield of 70%.[23] Although the heterogeneous catalyst demonstrated superior advantages in terms of catalyst recycling in comparison with homogeneous catalysts, the tedious recovery procedure *via* filtration or centrifugation and the inevitable loss of solid catalysts in the separation process still limited their application.

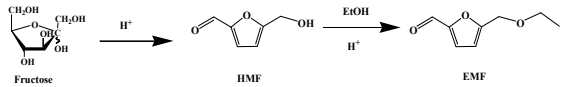

Scheme 1. Synthesis of EMF from fructose in ethanol.

Recently, magnetic nanoparticles (MNPs) have appeared as a new kind of catalyst support due to their good stability, and facile separation by magnetic forces.[24] The unique magnetic separation property makes MNPs much more effective than conventional filtration or centrifugation as it prevents loss of the catalyst. However, MNPs are readily aggregated due to the self interactions. In order to prevent the aggregation, the surface of MNPs was usually modified with silica layer, together providing a chemically inert surface for the chemical modification. The Keggin-type heteropoly acids such as $H_3PW_{12}O_{40}$ (HPW) have been extensively applied to catalyze many chemical reactions due to the high Brønsted acidity.[25, 26] Herein, in this study, driven by the excellent catalytic activity of $H_3PW_{12}O_{40}$ (HPW) and the unique magnetic separation property of Fe_3O_4, a magnetically-recoverable catalyst (Fe_3O_4@SiO_2-HPW) was prepared by the application of phosphotungstic acid (HPW) supported on silica-coated Fe_3O_4 nanoparticles (Fe_3O_4@SiO_2). Fe_3O_4@SiO_2-HPW was used to catalyze the synthesis of EMF from HMF and fructose with ethanol as the solvent. This new catalytic system possesses both high separation efficiency and a relatively high catalytic activity for the synthesis of a potential liquid fuel EMF from renewable resource.

2. Experimental Section

2.1 Materials and Methods

Keggin-type 12-tungstophosphoric acid was purchased from Aladdin Chemical Reagent Co., Ltd. (Shanghai, China). Aqueous NH_3 (28 wt.%), ethanol (99.5%), $FeSO_4.7H_2O$ (99.5 %), $FeCl_3.6H_2O$ (99.5 %), tetraethoxysilane (TEOS, 99.5%) and ethyl levulinate (99.0%) were purchased from Sinopharm Chemical Reagent Co., Ltd. (Shanghai, China), and ethanol (99.5%) was freshly distilled before use. 5-Hydroxymethylfurfural (98%) was supplied by Beijing Chemicals Co. Ltd. (Beijing, China). 5-Ethoxymethylfurfura (98%) was purchased from Hangzhou Imaginechem Co., Ltd. (Zhejiang, China). Fructose was purchased from Sanland-Chem International Inc. (Xiamen, China). Acetonitrile (HPLC grade) was purchased from Tania Co. Ltd. (Fairfield, USA). All other reagents were provided by local supplies (Wuhan, China) without further purification.

2.2 Preparation of the catalyst

2.2.1 Synthesis of Fe_3O_4

Fe_3O_4 was synthesized according to the known procedure by co-precipitation method.[27] $FeCl_3.6H_2O$ (2.703 g, 10 mmol) and $FeSO_4.7H_2O$ (1.390 g, 5 mmol) were dissolved in 50 mL of deionized water under vigorous mechanical stirring at 80 °C for 10 min under a nitrogen atmosphere. 8 mL of $NH_3.H_2O$ was added dropwise into the mixture solution for 5 min. Then 1 mL of 1M citric acid was added. After continuous stirring for 2 h, the magnetite precipitates were collected by a permanent magnet, and washed to pH = 7 using deionized water. Finally, the black precipitates were washed twice by ethanol and dried in vacuum at 70 °C overnight to obtain Fe_3O_4 nanoparticles.

2.2.2 Synthesis of Fe_3O_4@SiO_2

Firstly, Fe_3O_4 nanoparticles (2.0 g) was dispersed in a mixture solvent of ethanol (70 mL) and H_2O (10 mL) by sonication for 15 min. Then $NH_3.H_2O$ (5 mL) and TEOS (5.0 mL) were added successively. The mixture was stirred for 24 h under vigorous mechanical stirring. Then Fe_3O_4@SiO_2 precipitate was collected by a permanent magnet, and rinsed repeatedly with deionized water until the filter was neutral. Then Fe_3O_4@SiO_2 was washed with ethanol three times and dried in a vacuum.

2.2.3 Synthesis of Fe_3O_4@SiO_2-HPW

Fe_3O_4@SiO_2-HPW was prepared by a similar method which was used to support HPW on the surface of silica.[28] Fe_3O_4@SiO_2 (2.0 g) was firstly dispersed in 30 mL of deionized water by sonication for 30 min. Then an aqueous solution of HPW (0.8 g in 5mL of water) was added. After stirring for 24 h, the catalyst was collected by a permanent magnet, and washed three times with deionized water (20 mL ×3). Finally, the catalyst was dried at 100 °C for 12 h.

2.3 Catalyst characterization

Transmission electron microscope (TEM) images were obtained using an FEI Tecnai G^2-20 instrument. The sample powder were firstly dispersed in ethanol and dropped onto copper grids for observation. FT-IR measurements were recorded on a Nicolet NEXUS-6700 FTIR spectrometer with a spectral resolution of 4 cm^{-1} in the wave number range of 500-4000 cm^{-1}. X-ray powder diffraction patterns of samples were determined with a Bruker advanced D8 powder diffractometer (Cu Kα). The scan ranges were 10–80° with 0.016° steps, respectively. The content of W was determined by ICP/AES on an IRIS Intrepid II XSP instrument (Thermo Electron Corporation).

N_2 absorption-desorption experiment was carried out at −193 ºC using a Quantachrome Autosorb-1-C-MS instrument. The sample was subjected to be outgassed for 6 h at 200 ºC before the experiment. The surface area was obtained by using the BET method. The pore size was evaluated from the desorption branches of the isotherms by using the Barrett–Joyner-Halenda (BJH) method.

2.4 Titration of the catalyst acidity

The acidity of Fe_3O_4@SiO_2-HPW was probed by potentiometric titration.[29] Fe_3O_4@SiO_2-HPW (0.05 g) was suspended in acetonitrile, and stirred for 3 h. Then the suspension was titrated

with 0.05 M *n*-butylamine in acetonitrile at 0.05 ml/min. The electrode potential variation was measured with an Orion 420 digital A model by using a double-junction electrode.

2.5 Typical procedure for the synthesis of EMF

2.5.1 Synthesis of EMF from HMF

In a typical experiment for the synthesis of EMF from HMF, HMF (126 mg, 1 mmol) , Fe_3O_4@SiO_2-HPW (150 mg) and 5 mL of ethanol were charged in a 15-mL flask coupled with a reflux condenser under a nitrogen atmosphere, and the condenser was sealed with a balloon charged with nitrogen to avoid the release of ethanol during the reaction. The reactor was placed into a preheated oil bath kept at 100 °C and stirred magnetically at 600 rpm for a given reaction time. Time zero was taken when the reactor was immersed in the oil-bath heating device. Small aliquots were withdrawn from the reaction mixture at a given reaction time, and diluted with deionized water to a certain concentration for HPLC detective range. [30]

2.5.2 Synthesis of EMF from fructose

The reaction device was the same as the above for the synthesis of EMF from HMF. Firstly, fructose (180 mg, 1 mmol) was added into 5 mL of ethanol under stirring until a clear solution was formed. Then Fe_3O_4@SiO_2-HPW (150 mg) was added into the fructose solution. Time zero was taken when the catalyst was added into the reaction mixture. Otherwise steps were carried out in a similar way as the above description.

2.6 Determination of the products

Quantitative analyses of HMF and EMF were conducted on a ProStar 210 HPLC system using external standard calibration curve method. Samples were separated using a reversed-phase C18 column (200×4.6 mm) at 25 °C with a detection wavelength of 280 nm. Acetonitrile and 0.1 wt.% acetic acid aqueous solution (V:V = 15:85) were used as the mobile phase at a flow rate of 1.0 mL/min, and the column temperature was maintained at 303 K. The content of HMF and EMF in samples were obtained directly by interpolation from calibration curves, with a coefficient of 0.999.

The by-products such as ethyl levulinate was analyzed by gas chromatography (GC) on a 7890F instrument with a crosslinked capillary FFAP column (30 m × 0.32 mm × 0.4 mm) equipped with a flame ionization detector. Operating conditions were as follows: The flow rate of the N_2 carrier gas was 40 mL/min, the injection port temperature was 250 °C, the oven temperature was 190 °C, and the detector temperature was 280 °C. The peak of ethyl levulinate was identified by comparison of standard compound and quantified based on the internal standard method.

2.7 Recycling of catalyst

After reaction, the catalyst Fe_3O_4@SiO_2-HPW was seperated from the reaction mixture by a permanent magnet. Then the catalyst was washed three times with 10 mL of water, three times with 10 mL of ethanol, and dried at 100 °C in a vacuum oven over light.

3. Results and Discussion

3.1 Preparation and characterization of the catalyst

The magnetic nanoparticles (Fe_3O_4@SiO_2) supported HPW catalyst (Fe_3O_4@SiO_2-HPW) was prepared according to the following procedure, as shown in Scheme 2.

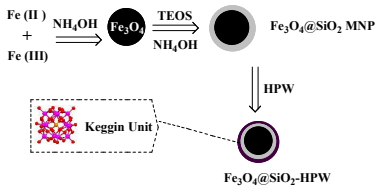

Scheme 2. Schematic illustration for the synthesis of Fe_3O_4@SiO_2-HPW.

The magnetic nanoparticles (MNP) Fe_3O_4 was easily prepared via co-precipitation method. Under a nitrogen atmosphere, an aqueous mixture of ferric and ferrous salts precipitated as an aqueous dispersion of Fe_3O_4 MNP via the addition of strong alkaline solutions of 28 wt. % $NH_3.H_2O$. Considering the aggregation tendency of the naked Fe_3O_4 MNP and acid corrosion problem, coating the magnetic nanoparticles with silica should be a good solution. Furthermore, the outer shell of silica also provides suitable sites (Si-OH groups) for surface functionalization with the precursor HPW. Fe_3O_4@SiO_2 MNP was obtained by the treatment of Fe_3O_4 with tetraethyl orthosilicate (TEOS) in an alkaline ethanol–water solution under strong alkaline conditions. Finally, HPW was immobilized on the support Fe_3O_4@SiO_2 to construct a magnetically-recoverable catalyst (Fe_3O_4@SiO_2-HPW). The XRD diffraction patterns of Fe_3O_4@SiO_2 and Fe_3O_4@SiO_2-HPW are shown in Fig. 1. The diffraction peaks in Fe_3O_4@SiO_2 and Fe_3O_4@SiO_2-HPW can be assigned to the planes of inverse cubic spinel structured Fe_3O_4, which match well with the standard Fe_3O_4 sample (JCPDS file No. 19-0629).[31] In addition, it should be pointed out that no separate crystal phase characteristic of bulk HPW existed in Fe_3O_4@SiO_2-HPW, which confirms the high dispersion of HPW on the support Fe_3O_4@SiO_2. [32]

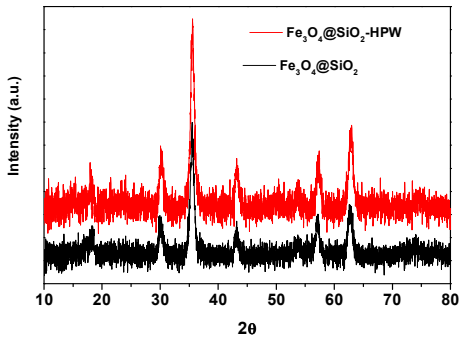

Fig. 1 XRD patterns of Fe_3O_4@SiO_2 and Fe_3O_4@SiO_2-HPW.

Transmission electron micrograph image of Fe_3O_4@SiO_2 NP is shown in Fig. 2. A typically core–shell structure of Fe_3O_4@SiO_2 NP was present. The dark core of the Fe_3O_4 and the grey silica shell were clearly observable. The typical silica shell thickness was assessed to be around 10 nm. However, some aggregations/coalescences of individual Fe_3O_4@SiO_2 appeared, and the aggregations might be performed during the coating process. The aggregations thus resulted in the form of bigger structures with a non-spherical morphology. We also tried to get a wide range of TEM containing three layers for Fe_3O_4@SiO_2-HPW, from which we would clearly seen a layer of HPW on the out surface of Fe_3O_4@SiO_2, but in vain. One important reason might be that the loading of HPW was low to give a distinct image in a wide rage. As detected by element analysis, the weight percentage of HPW was 26.8% in Fe_3O_4@SiO_2-HPW. In fact, Rafiee et al. prepared silica spheres supported HPW (Si-HPW), and Si-HPW was subjected to the TEM analysis.[33] Although the weight percent of HPW was reached 40 wt%, it could not observe a typical layer of HPW.

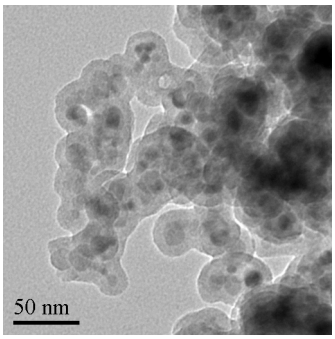

Fig. 2 Transmission electron microscope (TEM) image of Fe_3O_4@SiO_2

In order to further confirm the silica layer of Fe_3O_4@SiO_2 and the Keggin structure of HPW in Fe_3O_4@SiO_2-HPW, FT-IR was employed to give detailed structure of Fe_3O_4, Fe_3O_4@SiO_2 and Fe_3O_4@SiO_2-HPW. A band was presented around 1630 cm^{-1} for the three samples, which was attributed to adsorbed water.[34] The characteristic absorption band at 583 cm^{-1} was observed for Fe_3O_4 (curve a), which was due to the Fe–O vibrations.[35] In addition, a wide broad peak was also observed around 3400 cm^{-1}, which indicated that hydroxyl groups were presented on the surface of Fe_3O_4 MNP. In the case of Fe_3O_4@SiO_2 NP (curve 2), a band appeared at 1088 cm^{-1} was attributed to the Si–O–Si antisymmetric stretching vibrations, and the band at 800 cm^{-1} was also an evidence of the symmetric stretching vibration of the rocking mode of Si-O-Si. The presence of Si-OH symmetric stretching vibration was also confirmed by the absorption band at 950 cm^{-1}. The O–H stretching band around 3423 cm^{-1} were both presented in Fe_3O_4@SiO_2 and Fe_3O_4. Considering the FT-IR spectra of Fe_3O_4 and Fe_3O_4@SiO_2, it was clearly concluded that Fe_3O_4 was successfully coated with silica layer. It is well known that Keggin ion structure is consisted of a PO_4 tetrahedron, which is surrounded by four W_3O_9 groups formed by edgesharing octahedral.[36] There are four different types of oxygen atoms between 1100 and 500 cm^{-1}: oxygen atoms connected to three W atoms and P heteroatom (O_a), bridging oxygen atoms (O_b and O_c), and terminal oxygen atoms (O_d), which are responsible for the fingerprint bands of the Keggin ion. In the case of the spectra of Fe_3O_4@SiO_2-HPW, four kinds of oxygen atoms were stated as follows: P-O_a bands (1088 cm^{-1}), bridge W-$O_{b/c}$ bands (893 and 803 cm^{-1}), W-O_d bands (986 cm^{-1}), and the bending vibration of P-O (592 cm^{-1}), respectively. It should be pointed out that the band of P-O_a band was masked by the Si–O–Si absorption band in the FT-IR spectra of Fe_3O_4@SiO_2-HPW. The FT-IR spectra indicated that Keggin structure of HPW was maintained in Fe_3O_4@SiO_2-HPW. The content of W in the sample was determined to be 20.5%, indicated that a loading at *ca.* 26.8 wt% HPW was obtained.

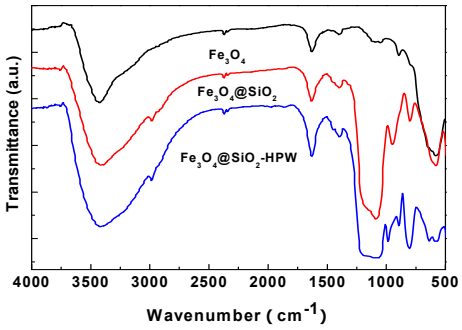

Fig. 3 IR spectra of (a) Fe_3O_4, (b) Fe_3O_4@SiO_2 and (c) Fe_3O_4@SiO_2-HPW.

Table 1. Textural properties of Fe_3O_4@SiO_2-HPW and Fe_3O_4@SiO_2

Sample	Surface area (m^2/g)	Pore volume (cc/g)	Pore size (nm)
Fe_3O_4@SiO_2	44.5	0.101	1.98
Fe_3O_4@SiO_2-HPW	27.6	0.064	1.85

In order to study the surface area and porous nature of the materials, the N_2 adsorption-desorption isotherms of Fe_3O_4@SiO_2 and Fe_3O_4@SiO_2-HPW were conducted. A typical isothermal of the Fe_3O_4@SiO_2 and Fe_3O_4@SiO_2-HPW samples are shown in Fig. 4. Isotherms of Fe_3O_4@SiO_2 and Fe_3O_4@SiO_2-HPW showed a type IV isotherm, and the samples were microporous material. With the loading of HPW, the hysteresis loop became shorter, corresponding to a reduction of pore volume. Table 1 shows values of BET surface area, pore size, and pore volume for Fe_3O_4@SiO_2 and Fe_3O_4@SiO_2-HPW. It was noted that Fe_3O_4@SiO_2 had much higher surface area and pore volume than Fe_3O_4@SiO_2-HPW. It seems logical as the loading of HPW was dispersed and deposited on the surface of Fe_3O_4@SiO_2, decreasing the pore diameter and thus diminishing the surface area.

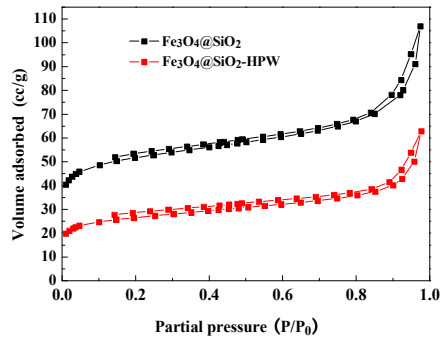

Fig. 4 Adsorption isotherm of Fe_3O_4@SiO_2 and Fe_3O_4@SiO_2-HPW.

3.2 Surface acidity measurements

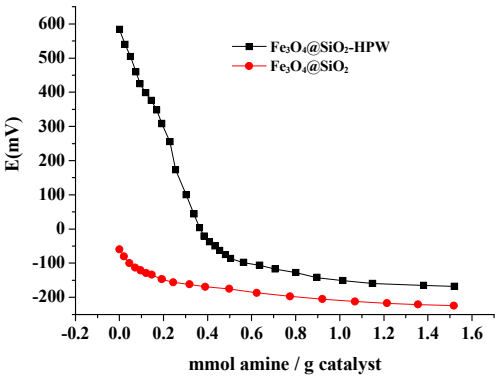

Fig. 5 Potentiometric titration of Fe_3O_4@SiO_2 and Fe_3O_4@SiO_2-HPW.

The acidity of Fe_3O_4@SiO_2-HPW was determined by a potentiometric titration method. This method is based on the measured potential difference, is mainly determined by the acidic environment around the electrode membrane. *n*-Butylamine is used as an organic base for the potentiometric titration of acid, which has a basic dissociation constant of approximately 10^{-6}. Using this technique, it was able to evaluate the strength of the acidity of Fe_3O_4@SiO_2-HPW. The potentiometric titration curves of Fe_3O_4@SiO_2 and Fe_3O_4@SiO_2-HPW are shown in Fig. 5. According to the previous references,[37] the initial electrode potential (Ei) indicated the maximum acid strength of the acid sites. The acid strength can be quantified according to the following scales: Ei > 100 mV (very strong sites), 0 < Ei < 100 mV (strong sites), −100 < Ei < 0 mV (weak sites) and Ei < −100 mV (very weak sites). As shown in Fig. 5, Fe_3O_4@SiO_2 showed a weak acid sites with an Ei value of -60 mV. The presence of Si-OH (silanol groups) on the surface of Fe_3O_4@SiO_2 are always weakly acidic in nature. The immobilization of HPW on the surface of Fe_3O_4@SiO_2 exhibited a very strong acidity with an Ei value of 584 mV. The strong acidity of Fe_3O_4@SiO_2-HPW was due to the replacement of the low acidity of silanol groups with stronger acidic sites of HPW, which caused an increase in the number and strength of the acid sites of Fe_3O_4@SiO_2-HPW.

3.3 Synthesis of EMF from HMF in the presence of various catalysts

The catalytic activity of Fe_3O_4@SiO_2-HPW was evaluated by the synthesis of EMF from the etherification of HMF. In order to evaluate the advantages of Fe_3O_4@SiO_2-HPW, various catalysts were employed to catalyze the etherification of HMF by ethanol (Table 2). No EMF was detected after reaction, when the reaction was carried out in the absence of catalyst (Table 2, Entry 1). In the meantime, negligible EMF yield of 0.2% was also noted in the presence of Fe_3O_4@SiO_2 (Table 2, Entry 2). However, the yield of EMF was largely increased to 76.9% with the HMF conversion of 89.5% when Fe_3O_4@SiO_2-HPW was used (Table 2, Entry 3). These results were in line with the results obtained by potentiometric titration. Taking the above results into consideration, HPW was the active catalytic species in Fe_3O_4@SiO_2-HPW for the synthesis of EMF from the etherification of HMF. HPW was also employed to catalyze the etherification of HMF. In order to give a reasonable comparison between HPW and Fe_3O_4@SiO_2-HPW, the amount of HPW was the same as the content of HPW in Fe_3O_4@SiO_2-HPW. HMF conversion and EMF yield with HPW as catalyst were close to those with Fe_3O_4@SiO_2-HPW as catalyst (Table 2, Entry 2 *vs* Entry 4). Unlike HPW, Fe_3O_4@SiO_2-HPW was insoluble in ethanol, but the catalytic activity was comparable with the homogeneous HPW. This was presumed to be due to the adsorption of reactants on the surface of the catalyst, increasing the local concentration of reactants around the active sites of the Fe_3O_4@SiO_2-HPW and promoted the reaction effectively. More importantly, a distinct disadvantage of the use of HPW was that the procedures for the catalyst recycling was complex, as HPW was dissolved in ethanol. In addition, two kinds of the representative solid catalysts were also studied for the synthesis of EMF. As expected, HMF conversion and EMF yield were low when the low acidity of HY-zeolite was used (Table 2, Entry 5). The sulfonated NKC-9 resin with a strong acidity could also effectively catalyze the etherification of HMF with the conversion of 93.3% and EMF was obtained in a yield of 78.8%. However, the structure of NKG-9 resin was destroyed seriously. The globose catalyst was pulverized after reaction, therefore catalyst recycling of NKG-9 resin was difficult. Xu et al. also reported the synthesis of EMF from the etherification of HMF catalyzed by MCM-41-supported $H_4SiW_{12}O_{40}$ catalyst, and an EMF yield of 77.3% was obtained, which was similar with our result (Table 2, Entry 7 *vs* Entry 3).[20] Meanwhile, the recycling experiments were carried out. Whereas, the recycling procedures for MCM-41-supported $H_4SiW_{12}O_{40}$were much more complex as compared with our magnetic Fe_3O_4@SiO_2-HPW catalyst. Considering all the above discussed results, Fe_3O_4@SiO_2-HPW not only had an appropriate acidity to promote the etherification

of HMF into EMF, but also was convenient in the catalyst recycling.

Table 2. Synthesis of EMF from HMF catalyzed by various catalysts.[a]

Entry	Catalyst	Catalyst amount (mg)	HMF Conversion (%)	EMF Yield (%)
1	-	-	0.3	0
2	Fe_3O_4@SiO_2	100	1.7	0.2
3	Fe_3O_4@SiO_2-HPW	100	89.5	76.9
4	$H_3PW_{12}O_{40}$	27	91.0	80.3
5[b]	HY-Zeolite	100	7.0	6.5
6	NKC-9 resin	100	93.3	78.8
7[b]	MCM-41-$H_4SiW_{12}O_{40}$	-	92.0	77.3

[a] Reaction conditions: a mixture of HMF (126 mg, 1 mmol) and catalyst were added into 5 ml of ethanol, and the reaction was carried out at100 °C for 11 h.

[b] Ref. 18. The reaction conditions: HMF (3 mmol), acid catalyst (0.051 mmol H^+), anhydrous ethanol (1.80 mL), oil bath at 90 °C for 2 h.

3.4 Effect of Fe_3O_4@SiO_2-HPW loading on the Synthesis of EMF from HMF

With the aim of optimizing the catalytic system, the effect of catalyst loading on the synthesis of EMF by the etherification of HMF was also studied. As shown in Fig. 6, HMF conversion and EMF yield were increased with the increase of the catalyst loading at the same reaction time point. Taking the reaction time of 1 h as an example, HMF conversions were reached in 10.1%, 28.6% and 38.6% with the catalyst loading at 50 mg, 100 mg, and 150 mg, respectively, and the corresponding EMF yields were 8.9%, 20.1% and 31.2%, respectively. An increase of HMF conversion and EMF yield with an increase of the catalyst loading could be attributed to an increase in the availability and number of catalytically active sites. When the reaction was stopped at 11 h, the maximum EMF yields were obtained in 71.7%, 76.9% and 83.6% with the amount of Fe_3O_4@SiO_2-HPW at 50 mg, 100 mg and 150 mg, respectively, corresponding to the conversion of HMF in 84.4%, 89.5% and 97.9%. Therefore 150 mg was selected as an appropriate catalyst loading in order to get a high EMF yield in the following experiments. It seems that the catalyst amount was a little high in order to get a high EMF yield. According to the elemental analysis, the weight percent of the supported HPW was 26.8%, thus 150 mg of Fe_3O_4@SiO_2-HPW was equaled to 40 mg of HPW. Although the catalyst Fe_3O_4@SiO_2-HPW could be readily recycled by a permanent magnet, it was necessary to develope a novel catalyst with a high catalyst activity to reduce the catalyst amount, which is potential in practical application for the synthesis of liquid fuel.

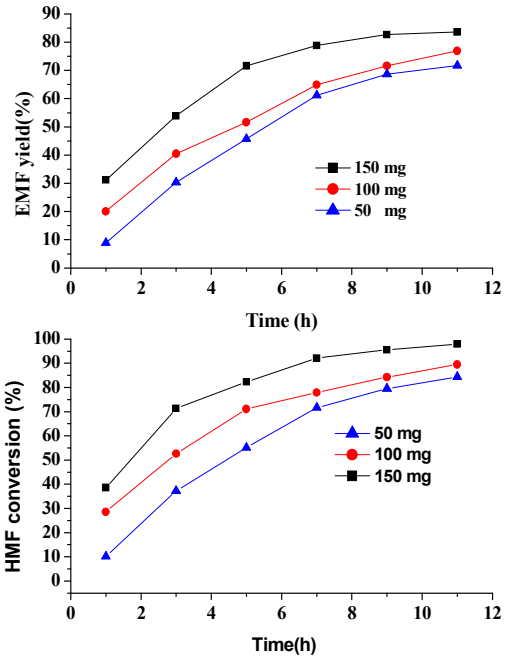

Fig. 6 The effect of catalyst loading on etherification of HMF catalyzed by Fe_3O_4@SiO_2-HPW in ethanol. Reaction conditions: HMF (126 mg, 1 mmol) and a set amount of Fe_3O_4@SiO_2-HPW were added into 5 mL of ethanol, and the reaction was carried out at 100 °C.

3.5 Synthesis of EMF from fructose

As the dehydration of fructose into HMF and the etherification of HMF into EMF are both acidic-catalyzed reactions, the integration of the two steps in one pot reaction is logically possible, which saves time and energy. Therefore, synthesis of EMF from fructose through one-pot reaction was carried out. As shown in Fig. 7, the reaction temperature had a remarkable effect on the yield of EMF. When the reaction was conducted at 70 °C, both HMF yield and EMF yield were rather low during the reaction process. EMF yield was slowly increased from 0.2% for 2 h to 5.2% for 24 h, and HMF yield was also kept at a low level. At the end of reaction, the conversion of fructose was detected to be 9.7%. The results indicated that the first step of the dehydration of fructose into HMF was difficult at 70 °C, but it was difficult to assess the followed etherification of HMF into EMF at 70 °C. Therefore, the etherification of HMF into EMF was also studied at 70 °C, as shown in Fig. 8. EMF yield was reached in 47.0% with HMF conversion of 53.6% for 11 h, indicating that the etherification reaction was relatively easier than the dehydration reaction.

EMF yield was largely increased from 2.8% for 2 h to 54.8% for 24 h when the one-pot reaction was carried out 100 °C. HMF yield was initially increased from 5.7% for 2 h to 10.8% for 8 h, and then it was kept at a stable level around 11%. Compared the results at 100 °C with those at 70 °C, the dehydration of fructose into HMF was promoted at a high reaction temperature. In addition, as HMF yield was almost stable from 8 h to 24 h, it was

concluded that the dehydration rate of fructose into HMF was close to the etherification rate of HMF. When the reaction temperature was further increased to 120 °C, EMF yield at the early stage was higher than that at 100 °C. Whereas, it was lower than that at 100 °C at the late stage. The maximum EMF yield at 120 °C was 41.9% for 24 h, which was lower than that at 100 °C. Fructose conversions were detected to be 94.7% and 100% for 24 h at 100 °C and 120 °C, respectively. In our experiment, the reaction mixture was analyzed by gas chromatography at the end of the reaction time of 24 h, and the yields of ethyl levulinate were determined to be 31.7% at 120 °C and 16.8% at 100 °C, respectively. These results indicated that the yield of ethyl levulinate was increased with the increase of reaction temperature. In general, the selectivity of EMF from fructose was much lower than that from HMF, which could be attributed to the following two reasons. On the one hand, dehydration of fructose into HMF was not effective in ethanol with Fe_3O_4@SiO_2-HPW as catalyst. On the other hand, some side reactions were presented such as the rehydration of HMF into levulinic acid.[38]

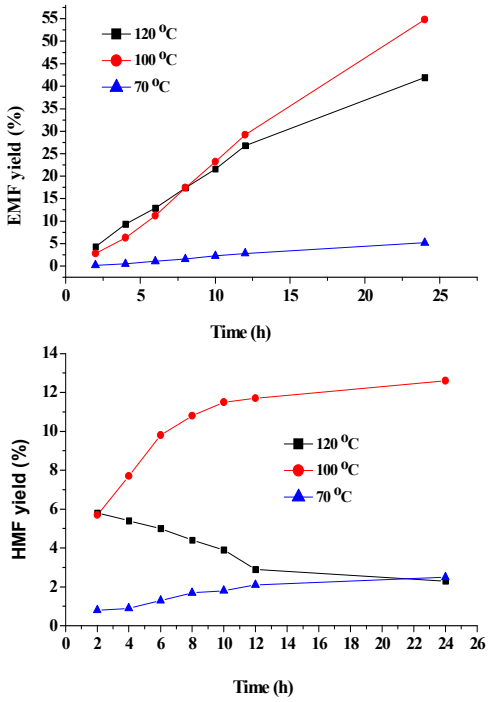

Fig. 7 Syntheis of EME from fructose catalyzed by Fe_3O_4@SiO_2-HPW at different reaction temperatures. Reaction conditions: Fructose (180 mg, 1 mmol) and Fe_3O_4@SiO_2-HPW (150 mg) were added into 5 mL of ethanol, then the reaction was carried out at desired temperature.

In order to give some insights into the difference between the synthesis of EMF at 100 °C and that at 120 °C, synthesis of EMF from HMF was also carried out at 100 °C and 120 °C, respectively. As shown in Fig. 8, HMF conversion was higher at 120 °C than that at 100 °C, but EMF yield at 120 °C was lower than that at 100 °C. HMF conversions were reached in 97.9% and 98.9% for 11 h at 100 °C and 120 °C, respectively, and the maximum EMF yields were obtained in 64.0% for 9 h at 120 °C and 83.6% for 11 h at 100 °C. Thus, the side reactions were much more serious at 120 °C than those at 100 °C. After reaction, the catalyst was removed from the reaction mixture by a permanent magnet, and some insoluble black humins were observed, which was formed by the polymerization and cross-polymerization of HMF.[39] On the other hand, ethyl levulinate as one of the major by-products was beneficially promoted at a high reaction temperature, which was caused by the alcoholysis of HMF. It was reported that ethyl levulinate could be reached in a high yield of 62% when HMF was treated in ethanol at 120 °C for 30 h in the presence of acid catalyst.[23] At the end of the reaction time of 11 h, ethyl levulinate yields were determined to be 26.3% at 120 °C and 5.8% at 100 °C, respectively. These results verified the major by-product for the synthesis of EMF from HMF was caused by the alcoholysis of HMF. It also indicated that ethyl levulinate yield was increased with the increase of reaction temperature. Other by-products such as humins and the self-etherification product [5,5'(oxy-bis(methylene))bis-2-furf ural] of two molecules of HMF was also quantified and the total carbon balance was calculated (ESI, Table 1)

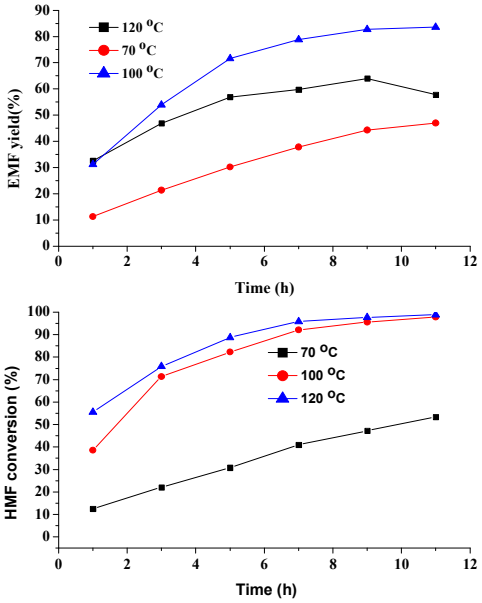

Fig. 8 Syntheis of EME from HMF catalyzed by Fe_3O_4@SiO_2-HPW at different reaction temperatures. Reaction conditions: HMF (126 mg, 1 mmol) and Fe_3O_4@SiO_2-HPW (150 mg) were added into 5 mL of ethanol, then the reaction was carried out at desired temperature.

3.6 Catalyst recycling experiments

The reuse of a catalyst is highly preferable in terms of green chemistry. Thus, the recycling experiments of Fe_3O_4@SiO_2-HPW were carried out by using the synthesis of EMF from HMF as a model reaction. After reaction, the reaction mixture was muddy (Fig. 9a). The catalyst Fe_3O_4@SiO_2-HPW could be easily

collected with the aid of a permanent magnet (Fig. 9b). Then liquid solution was removed from the mixture to leave the catalyst Fe_3O_4@SiO_2-HPW. Finally, the catalyst was washed by ethanol to remove the adsorbed products, dried under vacuum and reused in a subsequent reaction. Other catalytic cycles were repeated as described above. As shown in Fig. 10, in a test of six cycles, the catalyst could be reused without any significant loss of catalytic activity (83.2% in first cycle *versus* 78.8% in sixth cycle). In order to further verify the stability of Fe_3O_4@SiO_2-HPW during the reaction process, a control experiment was also carried out. Synthesis of EMF from HMF was firstly carried out at 100 ^oC in the presenc of Fe_3O_4@SiO_2-HPW for 3 h, then Fe_3O_4@SiO_2-HPW was removed from the reaction reaction mixture. The liquid mixture was continued to be stirred at 100 ^oC without Fe_3O_4@SiO_2-HPW. As shown in Fig. 11, EMF yield was stable after the removal of Fe_3O_4@SiO_2-HPW. These results once again verified Fe_3O_4@SiO_2-HPW was stable under our reaction conditions. The liquid mixture was subjetced to the elemental analysis by ICP-AES technology, and no W was detected, which also indicated that the supported HPW was not released into the reaction mixture from Fe_3O_4@SiO_2-HPW. We have also characterized the catalyst after reused for 6 times by FI-IR (ESI, Fig. S1) and XRD (ESI, Fig. S2). Compared the reused catalyst with the fresh catalyst, no distinct difference was observed.

In addition, the recycling experiments of the catalyst for the synthesis of EMF from fructose was also carried out, and EMF yields were kept stable around 54% for six runs (ESI, Fig S3). These results also indicated that the Fe_3O_4@SiO_2-HPW was stable. Incidentally, some silica supported HPW catalysts also showed high stability for the liquid organic reactions.[40] Whereas, it was also reported that the activity of some silica supported HPW catalysts was decreased during the recycling expriments. Liu et al., reported the toluene alklylation with 1-octene catalyzed by MCM-41 supported heteropoly acids, and found the catalytic acitivity was lost during the recycling expriments.[41] They considered that the catalyst after reaction could not be fully recovered by filtration, as the particle size was very small, leading to a loss of catalytic activity. Compared with the filtration method, the method for the recovery of the catalyt by a permanent magnet obviously avoids the catalyst loss during the recycling expriments (as shown in Fig. 9b).

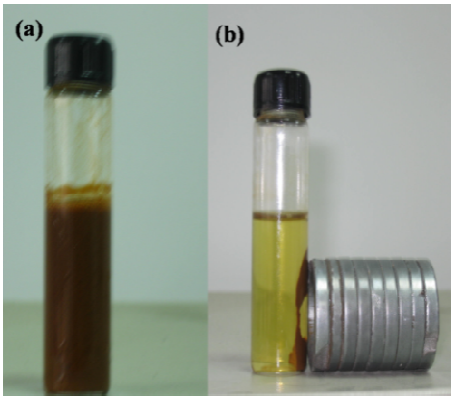

Fig. 9 Separation of the Fe_3O_4@SiO_2-HPW catalyst from the reaction mixture using an external magnet.

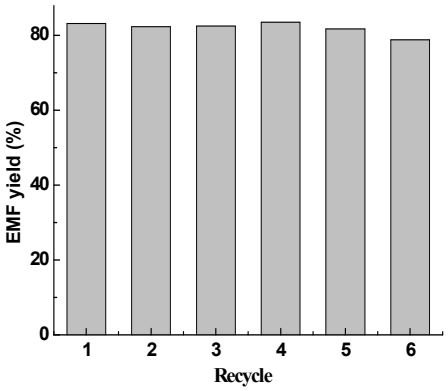

Fig. 10 Recycle experiments of the catalyst Fe_3O_4@SiO_2-HPW. Reaction conditions: HMF (126 mg, 1 mmol) and Fe_3O_4@SiO_2-HPW (150 mg) were added into 5 mL of ethanol, then the reaction was carried out at 100 ^oC.

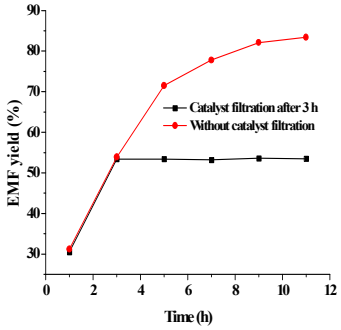

Fig. 11 The results of the control expriments after hot filtration for the synthesis of EMF from the etherification of HMF. Reaction conditions: HMF (126 mg, 1 mmol) and Fe_3O_4@SiO_2-HPW (150 mg) were added into 5 mL of ethanol, then the reaction was carried out 100 ^oC.

4. Conclusion

In conclusion, we have developed a novel magnetic Fe_3O_4@SiO_2 MNP supported heteropolyacid $H_3PW_{12}O_{40}$ catalyst for the synthesis of EMF from HMF and fructose. EMF was obtained with a high yield of 83.6% by the etherification of HMF, and a moderate EMF yield of 54.8% was also obtained from fructose through one-pot reaction. The special properties of HPW provided sufficient acidic sites for the excellent catalytic acitivity of Fe_3O_4@SiO_2-HPW. Moreover, Fe_3O_4@SiO_2-HPW could be readily removed from the reaction mixture by a permanent magnet, and it could be reused for several times without loss of its catalytic activity. In addition to the application for the synthesis of EMF, the environmentally benign catalyst Fe_3O_4@SiO_2-HPW would have a promising potential for other acid-catalyzed chemical reactions.

Acknowledgements

The Project was supported by National Natural Science Foundation of China (No. 21203252, 21206200), and the Special Fund for Basic Scientific Research of Central Colleges, South-Central University for Nationalities (CZY10006).

References

1 W. N. R. W. Isahak, M. W. M. Hisham, M. A. Yarmo, T. Y. Y. Hin, *Renew. Sust. Energ. Rev.*, 2012, **16**, 5910.

2 P. Anbarasan, Z. C. Baer, S. Sreekumar, E. Gross, J. B. Binder, H. W. Blanch, Harvey, D. S. Clark and F. D. Toste, *Nature*, 2012, **491**, 235.

3 K. Wilson and A. F. Lee, *Catal. Sci. Technol.,* 2012, **2,** 884.

4 S. Dutta, S. De, B. Saha and M. I. Alam, *Catal. Sci. Technol.,* 2012, **2,** 2025.

5 R. C. Baliban, J. A. Elia, C. A. Floudas, *Energy Environ. Sci.*, 2013, **6**, 267.

6 M. Chidambaram, A. T. Bell, *Green Chem.*, 2010, **12**, 1253.

7 S. Dutta, S. De, B. Saha, *ChemPlusChem*, 2012, **77**, 259.

8 R. Alamillo, M. Tucker, M. Chia, Y. Pagan-Torres, J. Dumesic, *Green Chem.*, 2012, **14**, 1413.

9 A. A. Rosatella, S. P. Simeonov, R. F. M. Frade and C. A. M. Afonso, *Green Chem*., 2011, **13**, 754.

10 H. Zhao, J. E. Holladay, H. Brown and Z. C. Zhang, *Science*, 2007, **316**, 1597.

11 Y. R. Leshkov, J. N. Chheda and J. A. Dumesic, *Science*, 2006, **312**, 1933.

12 J.B. Binder and R.T. Raines, *J. Am. Chem. Soc.*, 2009, **131**, 1979.

13 Z. H. Zhang, Q. Wang, H. B. Xie, W. J. Liu and Z. K. Zhao, *ChemSusChem*, 2011, **4**, 131.

14 V.V. Ordomsky, J. vander Schaaf, J. C. Schouten and T. A. Nijhuis, *J. Catal*., 2011, **287**, 68.

15 B. Liu, Z. H. Zhang and Z. K. Zhao. *Chem. Eng. J.*, 2013, **215-216**, 517.

16 M. Mascal and E. B. Nikitin, *Angew. Chem. Int. Ed*., 2008, **47**, 7924.

17 C. M. Lew, N. Rajabbeigi and M. Tsapatsis, *Ind. Eng. Chem. Res.,* 2012, **51**, 5364.

18 M. Mascal and E. B. Nikitin, *ChemSusChem,* 2009, **2**, 859.

19 P. Lanzafame, D. M. Temi, S. Perathoner, G. Centi, A. Macario, A. Aloise and G. Giordano, *Catal. Today*, 2011, **175**, 435.

20 P. H. Che, F. Lu, J. J. Zhang, Y. Z. Huang, X. Nie, J. Gao, J. Xu, *Bioresource Technol*., 2012, **119**, 433.

21 Y. Yang, M. M. Abu-Omar and C. W. Hu, *Appl. Energy* 2012, **99**, 80.

22 G. A. Kraus and T. Guney, *Green Chem*., 2012, **14**, 1593.

23 M. Balakrishnan, E. R. Sacia and A. T. Bell, *Green Chem*., 2012, **14**, 1626.

24 L. H. Reddy, J. L. Arias, J. Nicolas and P. Couvreur, *Chem. Rev*., 2012, 112, 5818.

25 R. Tayebee, F. Nehzat, E. Rezaei-Seresht, F. Z. Mohammadi and E. Rafiee, *J. Mol. Catal. A: Chem*., 2011, **351**, 154.

26 V.V. Costa, K.A.D. Rocha, I. V. Kozhevnikov, E. F. Kozhevnikova and E. V. Gusevskaya, *Catal. Sci. Technol.* 2013, 3, 244.

27 H. L. Ding , Y. X. Zhang, S. Wang , J. M. Xu , S. C. Xu , and G. H. Li, *Chem. Mater.*, 2012, **24**, 4572.

28 Y. Liu, L. Xu, B. B. Xu, Z. K. Li, L. P. Jia and W. H. Guo, *J. Mol. Catal. A: Chem.*, **2009**, 297, 86.

29 E. A. El-Sharkawy, A. S. Khder and A. I. Ahmed, *Micropor. Mesopor. Mater.*, 2007, **102**, 128.

30 B. Liu, Z. H. Zhang and K. J. Deng, *Ind. Eng. Chem. Res*., 2012, **51**, 15331.

31 J. Lee, Y. Lee, J. K. Youn, H. B. Na, T. Yu, H. Kim, S. M. Lee, Y. M. Koo, J. H. Kwak, H. G. Park, H. N., M. Hwang, J. G. Park, J. Kim and T. Hyeon, *Small*, 2008, **4**, 143.

32 A. Jha, A. C. Garade, S. P. Mirajkar and C. V. Rode, *Ind. Eng. Chem. Res.*, 2012, **51**, 3916.

33 E. Rafiee, M. Khodayari, S. Shahebrahimi and M. Joshaghani, *J. Mol. Catal. A: Chem.,* 2001, **351,** 204- 209.

34 I.V. Kozhevnikov, *Chem. Rev*., 1998, **98**, 171.

35 C. He, T. Sasaki, Y. Shimizu and N. Koshizaki, *Appl. Surf. Sci.*, 2008, **254**, 2196.

36 D. S. Pito, I. Matos, I. M. Fonseca, A. M. Ramos, J. Vital and J. E. Castanheiro, *Appl. Catal. A*, 2010, **373**, 140.

37 E. Rafiee, M. Joshaghani, S. Eavani and S. Rashidzadeh, *Green Chem*., 2008, **10**, 982–989.

38 R. Weingarten, W. C. Conner and G. W. Huber, *Energy Environ. Sci*., 2012, **5**, 7559.

39 S. J. Dee and A. T. Bell, *ChemSusChem*, 2011, **4**, 1166.

40 V. Brahmkhatri and A. Patel, *Fuel*, 2012, **102** , 72.

41 Y. Liu, L. Xu, B. B. Xu, Z. K. Li, L. P. Jia and W. H. Guo *J. Mol. Catal. A: Chem.,* 2009, **297**, 86.